

# Holographic Superconductors with the General $RF^2$ -type Couplings

Özcan Sert\*

Department of Mathematics, Faculty of Arts and Sciences, Pamukkale University  
20017 Denizli, Turkey

May 27, 2022

## Abstract

We explore the effects of the general non-minimally coupled  $RF^2$ -type couplings on the holographic s-wave superconductors numerically in the Schwarzschild-AdS background. We calculate the condensation and conductivity of the model for the coupling parameters  $a_1$  and  $\beta$ . We obtain that the bigger deviations of the parameter  $a_1$  from the minimal case lead to the larger deviations of the gap frequency from the universal value  $\omega_g/T_c \approx 8$ . Moreover the smaller  $\beta$  and  $a_1$  cause to gradually stronger and narrower coherence peak.

*PACS numbers:* 11.25.Tq, 03.50.De, 04.50.Kd

*Keywords:* Holographic superconductor; non-minimal couplings.

---

\*osert@pau.edu.tr

# 1 Introduction

The anti-de Sitter/conformal field theory (AdS/CFT) duality [1] provides a powerful relation between a theory of gravity in  $(d+1)$  dimensional AdS bulk space-time and a quantum field theory at the boundary of the bulk. On the boundary, basic properties of a  $d$ -dimensional superconductor such as; critical temperature, phase transition, can be reproduced by the  $(d+1)$ -dimensional holographic dual model[2, 3]. The model has a charged scalar field and an electromagnetic field as minimally coupled in an AdS background. An interesting extension of the minimal holographic model is to consider a non-minimal model which involves a term non-minimally coupled Weyl tensor and Maxwell field in the Lagrangian [4]-[9]. The model with the conformal invariant Weyl tensor is obtained from the special combination of the general  $RF^2$ -type model of this study:  $a_3 = \gamma/3$ ,  $a_1 = a_2 = \gamma$  and the others are zero. Another special combination of these non-minimal terms may be obtained from a five dimensional Gauss-Bonnet gravity via dimensional reduction [10]. Holographic properties of the later non-minimal model are investigated in Schwarzschild-AdS [11] and in the charged black hole background [12].

The general  $RF^2$ -type non-minimal models with vanishing scalar field and cosmological constant were considered to find solutions to the problems such as dark matter, dark energy, gravitational waves and primordial magnetic fields in the universe [13]-[20]. In the previous article [21], we have considered the holographic superconductor with arbitrary and perturbatively small coupling constants, and obtained a relation for critical temperature and condensation as approximate analytical solution. It is interesting to find how the description of the holographic superconductor change when we consider numeric solutions to this model.

In this study we investigate numeric properties of the non-minimal model with arbitrary coupling constants  $a_i$  and compare them with approximate analytic results in the probe limit. We obtain the effects of the coupling parameters  $a_i$  on the condensation of the scalar operators and conductivity.

## 2 The Non-minimal Model with Arbitrary Coupling Constants

We will give the model in terms of exterior differential forms. We denote orthonormal co-frames  $e^a$  and metric  $g = \eta_{ab}e^a \otimes e^b$  where  $\eta_{ab} = \text{diag}(-1, 1, 1, 1)$  is the Minkowski metric. The Hodge star  $*$  determines the orientation of space-time as  $*1 = e^0 \wedge e^1 \wedge e^2 \wedge e^3$ , where  $\wedge$  is the exterior product. The curvature 2-form is denoted by  $R^a{}_b$  and it is obtained from antisymmetric Levi-Civita connection 1-form as  $R^a{}_b = d\omega^a{}_b + \omega^a{}_c \wedge \omega^c{}_b$ . The interior product is denoted by  $\iota_a$  which satisfying  $\iota_b e^a = \delta_b^a$ , where  $\delta_b^a$  is the Kronecker symbol. Then the shorthand notations are used:  $\iota_a F = F_a$ ,  $\iota_b \iota_a F = F_{ab}$ ,  $\iota_a R^a{}_b = R_b$ ,  $\iota_b \iota_a R^{ab} = R$

We take the following Lagrangian density 4-form in differential form language:

$$\begin{aligned} \mathcal{L} = & \frac{1}{\kappa^2} [R_{ab} \wedge *e^{ab} + \Lambda *1 + (de^a + \omega^a{}_b \wedge e^b) \wedge \lambda_a] \\ & - \frac{1}{2} F \wedge *F - D\psi^\dagger \wedge *D\psi - m^2 \psi^\dagger \psi *1 \\ & + 2a_1 F^{ab} R_{ab} \wedge *F + 2a_2 F^a \wedge R_a \wedge *F + 2a_3 R F \wedge *F \\ & + 2a_4 F^{ab} R_{ab} \wedge F + 2a_5 F^a \wedge R_a \wedge F + 2a_6 R F \wedge F \end{aligned} \quad (1)$$

where  $\kappa$  is the gravitational coupling coefficient,  $a_i$ ,  $i = 1, 2, 3, 4, 5, 6$  are the non-minimal coupling coefficients and  $\Lambda$  is the cosmological constant. We will take the cosmological constant as  $\Lambda = 6/L^2$  in term of AdS radius  $L$ . In the Lagrangian,  $\lambda_a$  is Lagrange multiplier constraining connection to be Levi-Civita. The complex scalar field (hair) is denoted by  $\psi$  and covariant exterior derivative of it,  $D\psi = d\psi + iA\psi$ . The electromagnetic field is denoted by  $F = dA$ , which is exterior derivative of the electromagnetic potential 1-form  $A$ .

This Lagrangian is equivalent to the Lagrangian in [21] for  $a_i = c_i/4$  and  $a_4 = a_5 = a_6 = 0$ . If we set  $a_1 = a_3 = \alpha$ ,  $a_2 = 2\alpha$  and the others are zero, we obtain the  $RF^2$  corrected model which is investigated in [11].

In the probe limit, we have the electromagnetic field equation and the scalar field equation which is obtained from independent variations of the non-minimal Lagrangian according to  $A$  and  $\psi^\dagger$ , respectively,

$$\begin{aligned} d \left\{ 4a_1 * F^{ab} R_{ab} + 2a_2 [R_a \wedge \iota^a * F - R * F + *(F^a \wedge R_a)] + 4a_3 R * F - *F \right. \\ \left. + 4a_4 (F^a \wedge R_a + F_{ab} R^{ab}) + (2a_4 - 2a_5 + 4a_6) F R \right\} - 2|\psi|^2 * A = 0, \end{aligned} \quad (2)$$

$$D * D\psi - m^2\psi * 1 = 0. \quad (3)$$

It can be considered that  $\psi$  is real and have the mass  $m^2 = -2/L^2$ ; which is above the Breitenlohner-Freedman bound,  $m^2L^2 \geq -9/4$ . We look for solutions to the field equations in the background of a planar Schwarzschild-AdS metric:

$$g = -f(r)dt^2 + \frac{dr^2}{f(r)} + \frac{r^2}{L^2}(dx^2 + dy^2) \quad (4)$$

where

$$f(r) = \frac{r^2}{L^2}\left(1 - \frac{r_H^3}{r^3}\right). \quad (5)$$

We calculate the field equations (2) and (3) for the metric, the scalar field and electric potential 1-form which have only radial dependence  $\psi = \psi(r)$  and  $A = \phi(r)dt$ . Then we change the variable  $r$  to  $z$  using this relation  $z = r_H/r$ . Thus the outer region of the black hole  $r_H \leq r < \infty$  turns to the interval  $0 < z \leq 1$  in this new coordinates.

We look for solutions to the following differential equations which are obtained from (2) and (3):

$$\left[1 + \frac{8a_1}{\beta L^2}(1 - z^3)\right] \phi_{zz} - \frac{24a_1}{\beta L^2} z^2 \phi_z - \frac{2L^2}{\beta} \frac{\psi^2}{z^2(1 - z^3)} \phi = 0, \quad (6)$$

$$\psi_{zz} - \frac{2 + z^3}{z(1 - z^3)} \psi_z + \left[\frac{L^4 \phi^2}{r_H^2(1 - z^3)^2} + \frac{2}{z^2(1 - z^3)}\right] \psi = 0, \quad (7)$$

where  $\beta = 1 - 24a_2/L^2 + 48a_3/L^2$  and the subindex  $z$  denotes  $d/dz$ . We see that there is no contribution from the terms with  $a_4, a_5, a_6$  for the electromagnetic potential  $A = \phi(r)dt$ . We will take  $L = 1$  and  $r_H = 1$ , and focus first on the different numerical values on the coupling constants  $\beta$  and  $a_1$  to determine new properties of the general  $RF^2$ -type corrections.

In the limit  $z \rightarrow 0$ , the scalar field  $\psi$  and the electric potential function  $\phi$  will have the following asymptotic behavior:

$$\phi(z) = \mu - \rho z, \quad \psi(z) = \psi_1 z + \psi_2 z^2. \quad (8)$$

Here  $\mu$  is the chemical potential and  $\rho$  is the charge density on boundary.  $\psi_1$  and  $\psi_2$  are related to vacuum expectation value of the condensation and source operators in the field theory, that is  $\langle \mathcal{O}_1 \rangle$  and  $\langle \mathcal{O}_2 \rangle$ . Since the mass ( $m^2 = -2$ ) is near the BF bound, we choose either  $\psi_1 = 0$  or  $\psi_2 = 0$  [22]. We have also the regularity condition at the horizon  $z = 1$ :

$$\phi(1) = 0, \quad \psi_z(1) = \frac{2}{3}\psi(1). \quad (9)$$

We obtain numerical solutions of the general non-minimal  $RF^2$ -type holographic superconductors with the boundary conditions (8) and (9). In figures 1 and 2, we give the solutions of the condensates  $\langle \mathcal{O}_1 \rangle$  and  $\langle \mathcal{O}_2 \rangle$  depending on the relative temperature  $\frac{T}{T_c}$  for different  $\beta$  and  $a_1$ . The coupling constants  $a_2$  and  $a_3$  appears as the same combination  $1 - 24a_2 + 48a_3 = \beta$  in these differential equations (6), (7) and (13). Thus one can choose either  $a_2 = 0$  or  $a_3 = 0$  without loss of generality. In figure 1, the cases with  $\beta = 2.44, 1.96, 1.48, 1.24, 1, 0.76, 0.52, 0.28$  are obtained by setting  $a_2 = 0$  and  $a_3 = 0.03, 0.02, 0.01, 0.005, 0, -0.005, -0.01, -0.015$ , respectively. These values are chosen small for satisfying causality conditions. Similar to the previous findings on the holographic superconductors, the graphs show that the condensates  $\langle \mathcal{O}_1 \rangle$  and  $\langle \mathcal{O}_2 \rangle$  vanish as  $T \rightarrow T_c$ . Furthermore, the increase of  $\beta$  and  $a_1$  makes the condensation gap larger similar to the  $RF^2$  corrections in [11]. To increase  $\beta$ ,  $a_2$  must be decreased and/or  $a_3$  must be increased. Thus, while the coupling terms  $R_{ab}F^{ab} \wedge *F$  and  $RF \wedge *F$  increase the gap, the term  $R_a \wedge F^a \wedge *F$  decreases.

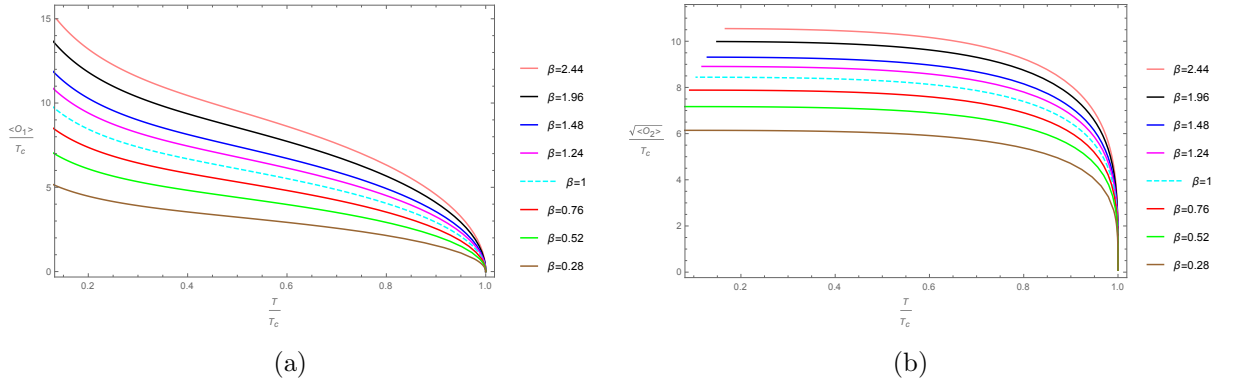


Figure 1: The condensates as a function of temperature: (a)  $\langle \mathcal{O}_1 \rangle$ , (b)  $\langle \mathcal{O}_2 \rangle$ , where  $a_1 = 0$ ,  $\beta = 2.44, 1.96, 1.48, 1.24, 1, 0.76, 0.52, 0.28$  from top to bottom and dashed line is  $\beta = 1$ .

On the other hand, we have the the following approximate analytical results which are obtained in [21] for  $\langle \mathcal{O}_2 \rangle$  >:

$$\langle \mathcal{O}_2 \rangle = \frac{80\pi^2}{9} \sqrt{\frac{2\beta}{3}} T T_c \sqrt{1 + \frac{T}{T_c}} \sqrt{1 - \frac{T}{T_c}} \quad (10)$$

(11)

where the critical temperature is

$$T_c = \frac{3\sqrt{\rho}}{4\pi L\alpha\sqrt{2\sqrt{7}}} \quad (12)$$

with  $\alpha^2 = 1 - 12a_1/(\beta L^2)$ . As we see from these approximate analytic results,  $\beta$  has an important effect for increasing the  $\langle \mathcal{O}_2 \rangle$  condensation gap, but  $a_1$  has not, which are consistent with the numerical solutions.

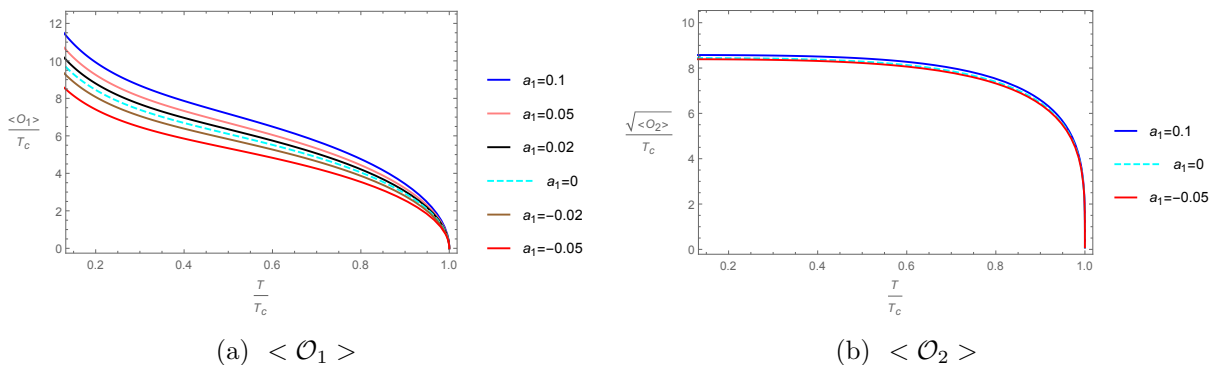


Figure 2: The condensates as a function of temperature in unit  $T_c$  for different  $a_1$ : (a)  $\langle \mathcal{O}_1 \rangle$ , (b)  $\langle \mathcal{O}_2 \rangle$ , where  $\beta = 0$ ,  $a_1 = 0.1, 0.05, 0.02, 0, -0.02, -0.05$  from top to bottom and dashed line is  $a_1 = 0$ .

The plots of the second case  $a_1 \neq 0$  and  $a_2 = a_3 = 0$  (or  $\beta = 1$ ) can be seen in figure 2. In this case,  $a_1$  has less effects on  $\langle \mathcal{O}_2 \rangle$  than  $\beta$  while they have more explicit effects on  $\langle \mathcal{O}_1 \rangle$ . We note that the condensates of the general  $RF^2$ -type model have similar behaviors with the condensates of the special combination of  $RF^2$  corrections in [11]. But these results are completely different from the effects of the Weyl corrections discussed in [4].

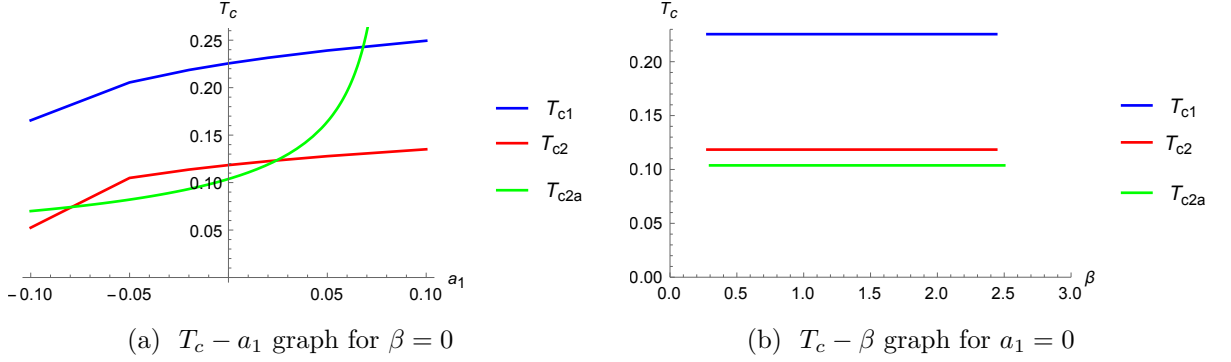


Figure 3: The numerical graphs of the critical temperature for the operators  $\langle \mathcal{O}_1 \rangle$  ( $T_{c1}$ ),  $\langle \mathcal{O}_2 \rangle$  ( $T_{c2}$ ), and the approximate analytical graph for  $\langle \mathcal{O}_2 \rangle$  ( $T_{ca}$ ).

A comparison of the numerical and approximate analytical results for the dependence of the critical temperature  $T_c$  to the coupling parameters  $\beta$  and  $a_1$  can be found in figure 3. The approximate analytic results deviate from the numeric solutions after  $a_1 = 0.05$ , excessively. This implies that there is an upper limit as  $a_1 < 1/12$  in the approximate analytic results. We see from figure 3-(a) the critical temperature  $T_c$  will increase as the coupling parameter  $a_1$  increases for the condensates. Thus the formation of scalar hair becomes more easier. But  $\beta$  does not have any important effect on the critical temperature for  $a_1 = 0$ , see figure 3-(b). However, when  $a_1 \neq 0$ , this situation of  $\beta$  will change. We give the formation of condensates in figure 4 for the last case.

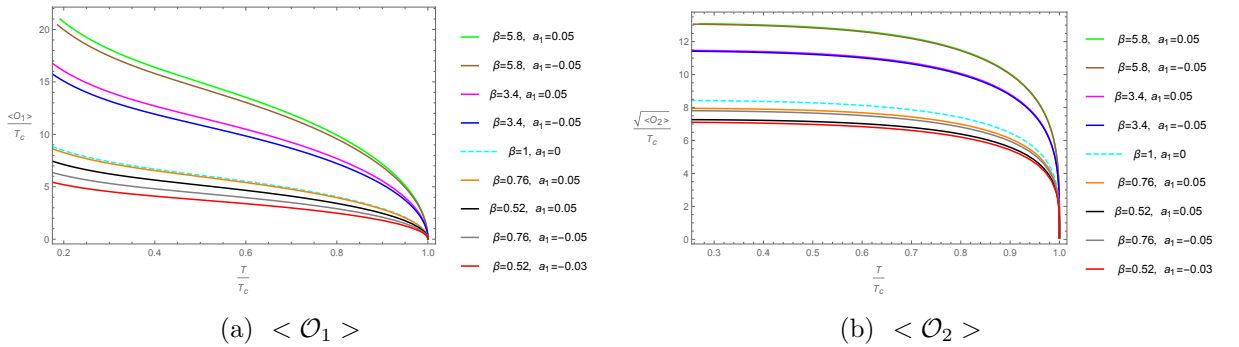


Figure 4: The condensates as a function of temperature for  $\langle \mathcal{O}_1 \rangle$  and  $\langle \mathcal{O}_2 \rangle$ . The condensation gap decrease as the parameters decreases from top to bottom.

### 3 Conductivity

In this section, we investigate electrical conductivity of the general non-minimal  $RF^2$ -type holographic superconductors. Since the current one-form  $J$  on the boundary is related with the Maxwell potential one-form in the bulk, we consider the perturbed Maxwell potential  $\delta A_x = A_x(r)e^{-i\omega t}dx$ , which has only x-component and find the following differential equation from Maxwell field equation:

$$\begin{aligned} & [\beta + 4a_1(z^3 + 2)] A_x'' + \left[ \frac{3\beta z^2}{z^3 - 1} + \frac{12a_1 z^2(2z^3 + 1)}{z^3 - 1} \right] A_x' \\ & + \left[ \frac{\beta\omega^2}{(z^3 - 1)^2} + \frac{4a_1\omega^2(z^3 + 2)}{(z^3 - 1)^2} + \frac{2\psi^2}{z^3 - 1} \right] A_x = 0 \end{aligned} \quad (13)$$

We have the following ingoing wave boundary condition near horizon ( $z=1$ ):

$$A_x(r) \sim f(r)^{-\frac{i\omega}{3r_+}} \quad (14)$$

and the asymptotic AdS boundary condition at  $z \rightarrow 0$ :

$$A_x = A^{(0)} + \frac{A^{(1)}}{r}. \quad (15)$$

The conductivity of the dual superconductor is calculated from

$$\sigma = -\frac{iA^{(1)}}{\omega A^{(0)}} \quad (16)$$

We calculate numerically the conductivities depending on the frequency  $\frac{\omega}{T_c}$  using (13), (7), (6) with the above boundary conditions. These results from the condensate  $\langle \mathcal{O}_2 \rangle$  are illustrated in figure 5 for different  $\beta$  values with  $a_1 = 0$  and for different  $a_1$  values with  $\beta = 1$ .



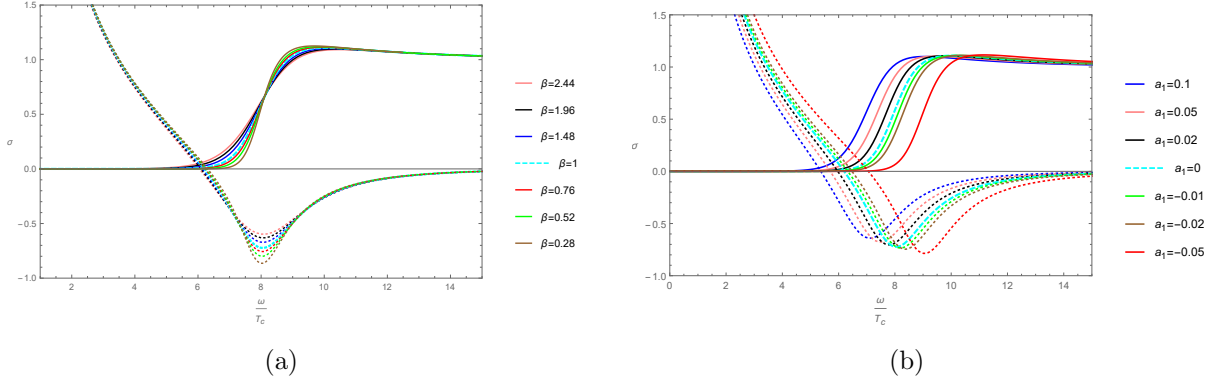


Figure 5: The conductivity as a function of frequency in unit of critical temperature for  $\langle \mathcal{O}_2 \rangle$ . While the solid lines represent the real part, the dotted lines represent the imaginary part of conductivity, and the dashed line (blue) is the case without non-minimal couplings ( $a_1 = 0$  and  $\beta = 1$ ) for  $T/T_c \approx 0.2$ .

In figure 5, we see that there is a gap in the conductivity with the gap frequency  $\omega_g/T_c$  and the gap rises quickly near the gap frequency which corresponds to the minimum of the imaginary part. Furthermore, the value of the gap frequency decreases (from right to left) as the parameter  $a_1$  increase (from bottom to top). But, while  $a_1 = 0$ ,  $\beta$  does not have any important effect on the value of the gap frequency and it has nearly the same gap frequency with the minimal coupling case ( $a_1 = 0$  and  $\beta = 1$ ), that is;  $\omega_g/T_c \approx 8$ . On the other hand, the effect of the smaller  $\beta$  or  $a_1$  is shown as gradually stronger and narrower the coherence peak.

These results support the previous findings obtained from the holographic models with the special  $RF^2$  correction in [11] and Weyl correction in [4]. This shows that the correction terms with  $a_1$ , will have important effects on the gap frequency for the strongly coupled model.

As we see the curves for  $\langle \mathcal{O}_2 \rangle$  in figure 6, there is another type of choice with  $a_1 \neq 0$  and  $\beta \neq 1$  in the conductivity. In this case the gap frequency has more shifts according to the case  $a_1 \neq 0$  and  $\beta = 1$ . The smaller  $\beta$  parameters lead to the bigger deviations for  $a_1 \neq 0$ , especially; for  $\beta < 1$ .

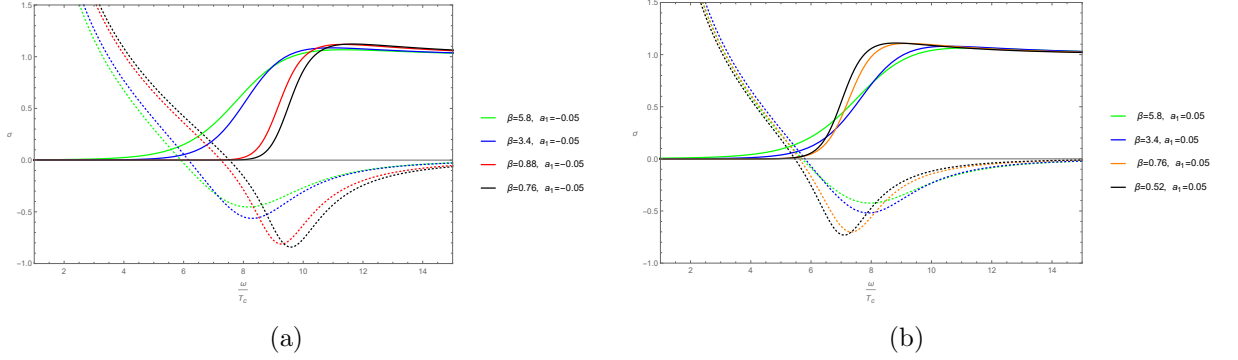


Figure 6: The conductivity which corresponds to the operator  $\langle \mathcal{O}_2 \rangle$  as a function of frequency in unit of critical temperature  $a_1 \neq 0$  and  $\beta \neq 1$ .

We have also plotted in figure 7 the real part of conductivity depends on the frequency which is in unit of the condensate. The curves from left to right which corresponds to the conductivity for decreasing beta values from top to bottom.

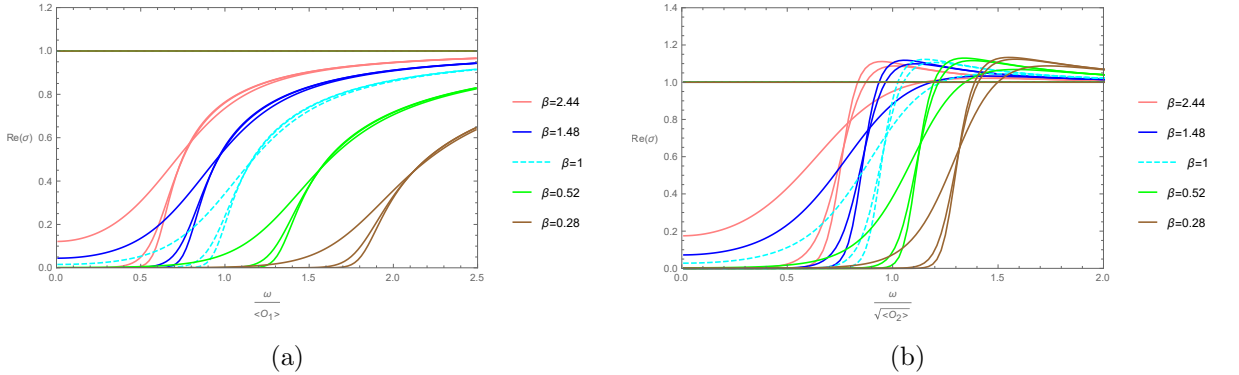


Figure 7: The real part of conductivity as a function of frequency with  $a_1 = 0$  and  $\beta \neq 0$  for  $\langle \mathcal{O}_1 \rangle$  (a) and  $\langle \mathcal{O}_2 \rangle$  (b).

In the table below, we give  $T/T_c$  values of the curves in figure 7 from left to right, respectively.

$\beta$	2.44	1.48	1	0.52	0.28
$(\frac{T}{T_c})_a$	0.67, 0.31, 0.20	0.57, 0.26, 0.16	0.50, 0.22, 0.14	0.39, 0.17, 0.11	0.31, 0.14, 0.09
$(\frac{T}{T_c})_b$	0.81, 0.36, 0.19	0.72, 0.27, 0.15	0.64, 0.22, 0.12	0.49, 0.16, 0.08	0.35, 0.11, 0.07

Table 1:  $\frac{T}{T_c}$  values,  $(\frac{T}{T_c})_a$  corresponds to the approximate values in figure 7(a) and  $(\frac{T}{T_c})_b$  in figure 7(b) from left to right for each  $\beta$ , respectively.

From this figure, we see that the horizontal lines in the real part of the conductivity represent the cases with the temperatures  $T \geq T_c$  and in these cases we can not observe any condensation. This corresponds to the normal phase of the AdS boundary while the conductivity has a gap for  $T < T_c$  which is superconducting phase. The gap in the conductivity and the coherence peak shifted from right to left with the increase of  $\beta$ . We have also found similar behaviors in the conductivity for changing  $a_1$  with  $\beta = 1$ .

## 4 Concluding remarks

We have investigated the general non-minimal  $RF^2$ -type holographic superconductors in the probe limit. We have found that the increase of the coupling parameter  $a_1$  leads to the higher critical temperatures while  $\beta = 1$  ( $a_2 = a_3 = 0$ ). But,  $\beta$  which is the combination of coupling parameters  $a_2$  and  $a_3$  does not give any contribution for higher critical temperature while  $a_1 = 0$ . There is another choice with  $a_1 \neq 0$  and  $\beta \neq 1$ . In this case,  $\beta$  also have important effects for higher critical temperatures. We have shown that the higher correction terms with  $a_1$  and  $\beta$  lead to the larger condensates  $\langle \mathcal{O}_1 \rangle$  and  $\langle \mathcal{O}_2 \rangle$ . These results are consistent with the findings for  $\langle \mathcal{O}_2 \rangle$  in the approximate analytical calculations [21].

We also calculated the conductivity of the general  $RF^2$ -type holographic superconductors. We found that the parameter  $a_1$  has more effect on the gap frequency than  $\beta$ . Furthermore,  $\beta$  and  $a_1$  change the strength and amount of the conductivity and coherence peak.

In figure 6, we saw the another type of choice with  $a_1 \neq 0$  and  $\beta \neq 1$ , and found the gap frequency has more shifts from the case with only  $a_1 \neq 0, \beta = 1$  or  $\beta \neq 1, a_1 = 0$ . The smaller  $\beta$  parameters lead to the bigger deviations for the values  $a_1 \neq 0$ . These results support the previous findings obtained from the holographic models with the special  $RF^2$  correction in [11] and Weyl correction in [4]. This shows that the non-minimal corrections change the universal gap frequency.

## Acknowledgement

This work is supported by the Scientific Research Project (BAP) 2016HZDP023, Pamukkale University, Denizli, Turkey.

## References

- [1] J. Maldacena, *Adv. Theor. Math. Phys.* **2**, 231 (1998) [*Int. J. Theor. Phys.* **38**, 1113 (1999)]
- [2] S. A. Hartnoll, C. P. Herzog and G. T. Horowitz, Building an AdS/CFT superconductor, *Phys. Rev. Lett.* **101** (2008) 031601 [arXiv:0803.3295]
- [3] S. A. Hartnoll, C.P. Herzog and G. T. Horowitz, *JHEP* **12** 015 (2008) [arXiv:0810.1563]
- [4] J. P. Wu, Y. Cao, X. M. Kuang, and W. J. Li, *Phys. Lett. B* **697**, 153 (2011)
- [5] D. Z. Ma, Y. Cao, and J. P. Wu, *Phys. Lett. B* **704**, 604 (2011)
- [6] D. Momeni, N. Majd, and R. Myrzakulov, *Europhys. Lett.* **97**, 61001 (2012)
- [7] D. Roychowdhury, *Phys. Rev. D* **86**, 106009 (2012)
- [8] D. Momeni, M. R. Setare, and R. Myrzakulov, *Int. J. Mod.Phys. A* **27**, 1250128 (2012)
- [9] Z. Zhao, Q. Pan, and J. Jing, *Phys. Lett. B* **719**, 440, (2013)
- [10] R.C. Myers, S. Sachdev, and A. Singh, *Phys. Rev. D* **83**, 066017 (2011)
- [11] Z. Zhao, Q. Pan, S. Chen and J. Jing, *Chinese Phys. Lett.* **30**, 121101 (2013)
- [12] R.G. Cai and D.W. Pang, *Phys. Rev. D* **84**, 066004 (2011)
- [13] I. T. Drummond and S. J. Hathrell, *Phys. Rev. D* **22** 343 (1980)
- [14] T. Dereli and G. Üçoluk, *Class. Q. Grav.* **7** 1109 (1990)
- [15] G. Lambiase, S. Mohanty and G. Scarpetta, *JCAP* **07** 019 (2008)

- [16] K. Bamba, S. Nojiri and S. D. Odintsov, *JCAP* **10** 045 (2008) [arXiv:0807.2575]
- [17] K. E. Kunze *Phys. Rev. D* **81** 043526 (2010) [arXiv:0911.1101]
- [18] T. Dereli and Ö. Sert, *Phys. Rev. D* **83** 065005 (2011) [arXiv:1101.1177]
- [19] T. Dereli and Ö. Sert, *Mod. Phys. Lett. A* **26** 1487 (2011) [arXiv:1105.4579]
- [20] Ö. Sert, M. Adak, An anisotropic cosmological solution to the Maxwell-Y(R) gravity  
arXiv:1203.1531 [gr-qc]
- [21] Ö. Sert, M. Adak, *Mod. Phys. Lett. A* 28, 40, 1350190, (2013)
- [22] S. S. Gubser, *Phys. Rev. D* 78, 065034 (2008)